ACS Sustainable Chemistry & Engineering

Research Article

pubs.acs.org/journal/ascecg

Bifunctional Peppermint Oil Nanoparticles for Antibacterial Activity and Fluorescence Imaging

Mei-Lang Kung,[†] Pei-Ying Lin,[†] Chiung-Wen Hsieh,[†] Ming-Hong Tai,[‡,§,¶] Deng-Chyang Wu,[∥,⊥,#,¶] Chao-Hung Kuo,[∥,⊥,#,¶] Shu-Ling Hsieh,[▽] Hui-Ting Chen,[○] and Shuchen Hsieh*[,†,◆,¶]

[†]Department of Chemistry, National Sun Yat-sen University, 70 Lien-hai Rd., Kaohsiung, Taiwan 80424, Republic of China

[‡]Department of Medical Education and Research, Kaohsiung Veterans General Hospital, Kaohsiung, Taiwan 81362, Republic of China

[§]Institute of Biological Science, National Sun Yat-sen University, Kaohsiung, Taiwan 80424, Republic of China

[¶]Center for Stem Cell Research, Kaohsiung Medical University, Kaohsiung, Taiwan 80708, Republic of China

[∥]Division of Gastroenterology, Department of Internal Medicine, Kaohsiung Medical University Hospital, Kaohsiung, Taiwan 80708, Republic of China

[⊥]Department of Medicine, College of Medicine, Kaohsiung Medical University, Kaohsiung, Taiwan 80708, Republic of China

[#]Cancer Center, Kaohsiung Medical University Hospital, Kaohsiung, Taiwan 80708, Republic of China

[▽]Department of Seafood Science, National Kaohsiung Marine University, Kaohsiung, Taiwan 81157, Republic of China

[○]Department of Fragrance and Cosmetic Science, Kaohsiung Medical University, Kaohsiung, Taiwan 80708, Republic of China

[◆]School of Pharmacy, College of Pharmacy, Kaohsiung Medical University, Kaohsiung, Taiwan 80708, Republic of China

Supporting Information

ABSTRACT: Essential oil from peppermint plants was used to prepare luminescent nanoparticles via a simple, one-step, thermal synthesis process. The peppermint oil nanoparticles (NPs) had a narrow particle size distribution (1.5 ± 0.5 nm) with prominent blue emission under UV irradiation. Photoluminescence (PL) spectra of the peppermint oil NP dispersion exhibited characteristic emission peaks when excited from 350 to 540 nm. The characteristic fragment from GC/MS shows the peppermint oil contains various components with antimicrobial activities. These components underwent conversion while forming the NPs via heat treatment. Transmission Fourier transform infrared (FTIR) spectra and X-ray photoelectron spectroscopy (XPS) were used to characterize the NP chemical composition, and revealed that functional groups, such as C═O, C−O, and −CH, were present on the NP surfaces, which could act as fluorescent emissive traps. Additionally, the NPs exhibited strong antimicrobial efficiency and demonstrated good fluorescent emission during bacteria imaging, making them good candidates as antibacterial agents and multifluorescence tracers for bacterial disease treatment.

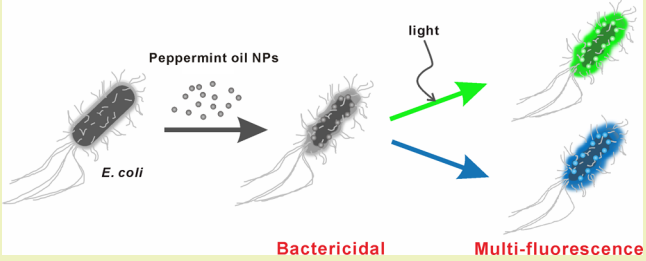

KEYWORDS: *Bactericidal, Multifluorescence, Atomic force microscope, Bioimaging, Essential oil*

INTRODUCTION

Nanomedicine is a rapidly growing field of research that strives to address biological questions and problems from a nanoscale-centric viewpoint.[1,2] Nanparticles (NPs) are an important subset of this emerging discipline with the traditional uses of sensing,[3] imaging,[4] and drug delivery,[2] being further advanced to include, for example, antimicrobial activity.[5,6] Several metallic nanoparticles and their derivatives, such as Au, Ag, ZnO, CuO, Fe_2O_3, etc., have been effectively used as antibacterial agents against Gram-positive and Gram-negative bacteria.[5−7] Quantum dots (QDs) have also been shown to exhibit antibacterial properties.[8,9] Lu et al. demonstrated that CdTe QDs can kill bacteria in a concentration-dependent manner with excellent optical properties.[9] Luo et al. further suggested a method to dynamically monitor bacteria concentration based on fluorescence detection.[10] However, these materials can be costly and hazardous; thus, a readily available low toxicity substitute is needed.

Due to the spread of multidrug-resistant pathogens and its serious threat to public health, interest in the antibacterial activity of essential oils has grown.[11,12] Essential oils, particularly those extracted from aromatic plants, have well-known antibacterial, antimicrobial, and insecticidal properties in various therapeutic uses.[13,14] Some essential oils have even shown antidiabetic,[15] anti-inflammatory,[16] or anticancer activity.[17,18] Although essential oils exhibit a wider range of application over antibacterial nanoparticles, the optical properties of essential oils and their

Received: December 2, 2013
Revised: May 13, 2014
Published: May 23, 2014

constituents have thus far received very little investigation. Recently, it was reported that the luminescent emission of Wild Camomile oil was detected on the skin of mice.[19] This demonstrates that some essential oils have luminescent properties and may have potential as specific biomarkers. Further, because they are nontoxic and readily available, some essential oils may be attractive alternatives to replace conventional QDs for biomedical applications.

Peppermint is one of the most well-known herbs for its wide medicinal uses as well as its multifunctional properties including antibacterial, antifungal, antiviral, and anti-inflammatory activity. In addition, it has been shown that peppermint oil exhibits visible fluorescence, making it a strong candidate as a bifunctional agent for bactericidal and bioimaging applications.[20] In the present study, we investigate the use of peppermint oil nanoparticles as a new type of fluorescent label and bactericidal agent for pathogenic bacteria.

EXPERIMENTAL SECTION

NP Synthesis. Peppermint oil (BIO−DIÄT Berlin GmbH, Germany) was used without further purification. All glass vials were cleaned using surfactant solution (Extran MA02 neutral, Merck, Darmstadt, Germany) followed by rinsing with ethanol and water (Millipore, Milford, MA, U.S.A.) and then dried in the oven at a constant temperature of 100 °C. A total of 2 mL aliquot was placed into thoroughly cleaned glass vials and held at a constant temperature of 120 °C on a hot plate (Suntex Inc. Co., Taiwan, SH-301) using heat-stirring (1100 rpm) for 1 h in an ambient air atmosphere and then stir-cooled to room temperature. Finally, the heat-treated peppermint oil solution was passed through a 0.45 μm polyvinylidene fluoride (PVDF) syringe filter (Millipore Millex-HV). This stock solution was then used to prepare samples for characterization by PL, XPS, and FTIR analysis.

Nanoparticle Characterization. Nanoparticle samples were prepared for atomic force microscopy (AFM) analysis by diluting the stock solution with methanol at a 1:1000 V/V ratio, drop-casting a 3 μL aliquot of the diluted solution onto mica surfaces at room temperature and allowing them to dry. Topographic images were acquired in AC mode using an AFM (MFP-3D, Asylum Research, Santa Barbara, CA, U.S.A.) under ambient conditions. A silicon cantilever (Olympus AC240TS) with a nominal spring constant of 2 N m^{-1} was used for all images, with a scan rate of 1.0 Hz and an image resolution of 512 pixel × 512 pixel.

Photoluminescence (PL) spectra of the NP stock solution were acquired using a HITACHI F-4500 fluorescence spectrometer. The excitation wavelengths were 300 to 500 nm at 20 nm intervals in the excitation domain. Emission spectra were recorded from 200 to 800 nm.

The GC/MS system consisted of a Trace GC2000 (Thermo Finnigan, U.S.A.) and a Trace MS detector (Thermo Finnigan, U.S.A.). Peppermint oil and peppermint oil NPs were diluted in methanol at 1:200 V/V, and 0.4 μL was injected into an HP-5MS column [low bleed (5%)-diphenyl-(95%)-dimethylsiloxane copolymer; dimensions 30 m × 0.25 mm × 0.25 μm]. The GC/MS inlet temperature was maintained at 250 °C, and the carrier gas was helium at a flow rate of 1 mL/min. The splitless mode was employed. The temperature program used was as follows. The temperature was kept at 75 °C for 1 min and then elevated at a rate of 10 °C/min up to 275 °C. The MS worked in selected-ion monitoring (SIM) mode, and the electron impact energy was set at 70 eV (Ion Source Temp. 200 °C).

X-ray photoelectron spectroscopy (XPS) was used to investigate the elemental composition of peppermint oil NPs using a JEOL JPS 9010 MX equipped with a monochromatic Mg Kα X-ray radiation source. Samples were prepared for XPS by depositing an aliquot of peppermint oil NP solution onto clean silicon substrates at room temperature. We used Fityk (0.9.8), an open-source spectra modeling program, for peak fitting. The intensity and position of the peaks corresponding to the C−O, C═O, and −COO bonds in these mixtures were quantified by fitting Gaussian functions to features in the pair distribution function within Fityk.

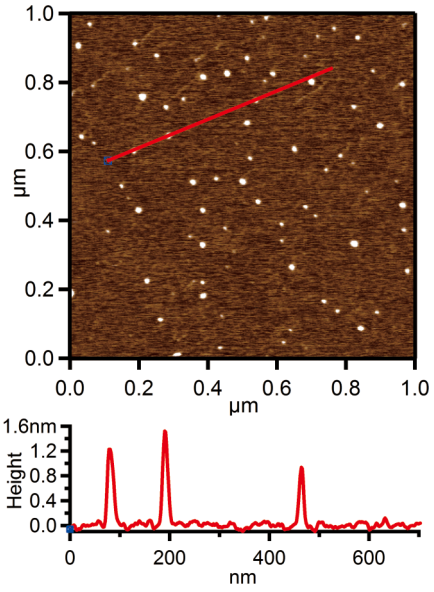

Figure 1. AFM topographic image (1 μm × 1 μm) of peppermint oil NPs deposited on mica. The red line in the image indicates where the corresponding line section (bottom graph) was acquired.

Transmission Fourier transform infrared (FTIR) spectra were acquired (8 cm^{-1} resolution, 256 scans, sample compartment vacuum pressure of 0.12 hPa) using a Bruker 66 v/s FTIR spectrometer. A double side polished silicon (100) wafer substrate was cut into 20 mm × 20 mm pieces with a diamond-tipped stylus. A droplet of the diluted peppermint oil NP solution (10 μL) was drop-cast onto the substrate, which was then mounted horizontally on the spin-coating machine at 3000 rpm for 2 min. A spectrum from a freshly plasma-cleaned silicon wafer sample was collected before each measurement to obtain the background spectrum.

Bacterial Colony Experiment. Microbial strains of *E. coli* were cultured in 50 mL of Luria−Bertani (LB) broth. After incubation overnight at 37 °C (OD570 0.57; cfu count 1.3 × 10^9 per mL), the bacterial cells (1 mL) were centrifuged for 5 min at 6000 rpm. For the aerobic plate determination, the bacteria were washed twice with a sterilized phosphate buffered saline (PBS) at pH 7.4 and then resuspended in PBS under gentle vortex mixing. Peppermint control or nanoparticles were premixed with glycerol at a 1:1 ratio and then placed into each group at a final concentration of 5%, 10%, and 25%, respectively. These assay groups were shaken at 25 °C for 3 h and then harvested for subsequent experiments. For the three-phase streaking pattern assay, the bacteria were directly streaked onto the agar plate and incubated at 37 °C for 16 h; the bacteria streaking patterns were imaged using an inverted optical microscope. For colony formation assay, these assay groups were washed twice and adequately diluted with PBS; bacteria were then inoculated onto nutrient agar plates and incubated at 37 °C for 16 h. The numbers of colonies formed was counted and recorded.

Fluorescence Microscopy. Fluorescence microscopy was used to assess the fluorescent labeling capability of peppermint oil NPs using *E. coli* cells prepared and suspended in PBS (1.0 × 10^8 per mL). Peppermint oil or nanoparticles were premixed with glycerol at a 1:1 ratio, and then each was placed into a group at a final concentration of 10%. A glycerol control sample was also tested. The samples were mixed well using a vortexer (VORTEX-2 GENE), and each group was kept at 25 °C and 155 rpm for 3 h. These samples were subsequently washed twice with PBS, and the images were recorded using a fluorescence microscope (DM 6000B, Leica, Germany). Blue fluorophores, λex = 359 nm, were detected with a 461 nm DAPI filter. Green fluorophores, λex = 499 nm, were detected with a 520 nm FITC filter.

Antibacterial Activity of Peppermint Oil NPs. The antibacterial activity of the peppermint oil NPs was validated using the Kirby−Bauer disc diffusion test. A bacterial suspension (10^8 CFU/ml) was swabbed

onto LB Agar plates. Eight millimeter diameter sterile discs (Whatman, U.S.A.) were impregnated with one of three different components: glycerol, peppermint oil, and synthesized peppermint oil NPs at concentrations of 5%, 10%, and 25% at 30 μL/disc. Kanamycin was used as a positive control. The discs were gently pressed and incubated at 37 °C for 24 h. The diameter of the zone of inhibition for each disc was measured in millimeters using a zone measuring scale. The experiments were executed in triplicate.

RESULTS AND DISCUSSION

Structural and Optical Characterization. The peppermint oil NP structure and size were characterized using AFM.

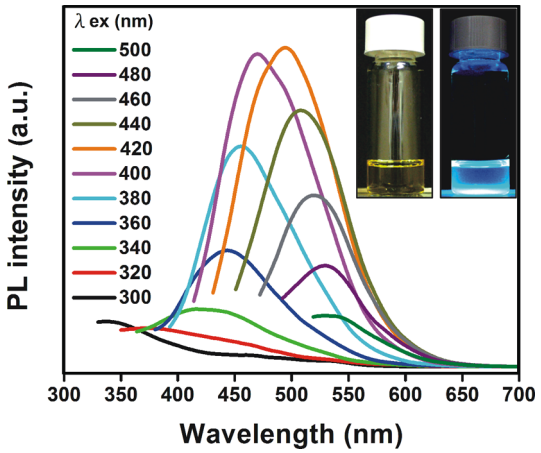

Figure 2. PL spectra of peppermint oil NPs. A stock sample solution was analyzed at progressively longer excitation wavelengths from 300 to 500 nm in 20 nm increments. The inset shows digital photographs of peppermint oil NP solutions under visible (left), and under 365 nm UV irradiation (right).

Figure 1 shows a topographic image (1 μm^2 scan) and a single line section profile of NPs deposited on a freshly cleaved mica substrate. The AFM images show that the NPs are essentially spherical and are well-dispersed on the mica surface. The average diameter of the NPs was 1.5 ± 0.5 nm, as determined by histogram analysis of the measured heights of 75 NPs in the image (Figure S1, Supporting Information). This small size of the peppermint oil NPs is important for potential applications, where it has been shown that NP diameters <5.5 nm minimize steric effects and can result in rapid urinary excretion and renal clearance from the body in biomedical applications.[21]

Photoluminescence spectra characterization of peppermint oil NPs was carried out at several excitation wavelengths, from 300 to 500 nm. As shown in Figure 2, the emission spectra from peppermint oil NPs was broad, ranging from 350 (violet) to 540 nm (green), and exhibited a peak-maximum wavelength dependence on the excitation wavelength. The PL spectrum of peppermint oil NPs excited by a 420 nm laser, for example, had an emission peak maximum at 495 nm. Further, the NP solution exhibited strong blue visible emission under UV irradiation as shown in the inset of Figure 2. These results are consistent with similar behavior observed for other types of NPs and nanodots where particle size,[22] surface emissive traps,[23,24] and aromatic conjugate structures[25] are thought to contribute to bright and multicolor fluorescence under UV and visible irradiation.

The GC/MS chromatogram analysis of peppermint oil exhibited five main peaks, including 1,8-cineole (10.7%), menthone (25.9%), menthol (44.9%), pulegone (9.7%), and caryophyllene (2.6%), as shown in Figure 3a I–V, respectively. This composition is in agreement with previous literature reports.[26] Conversion of these components occurred while peppermint oil was heated to form NPs, resulting in the generation of three new compounds (Figure 3b VI–VIII). We propose that

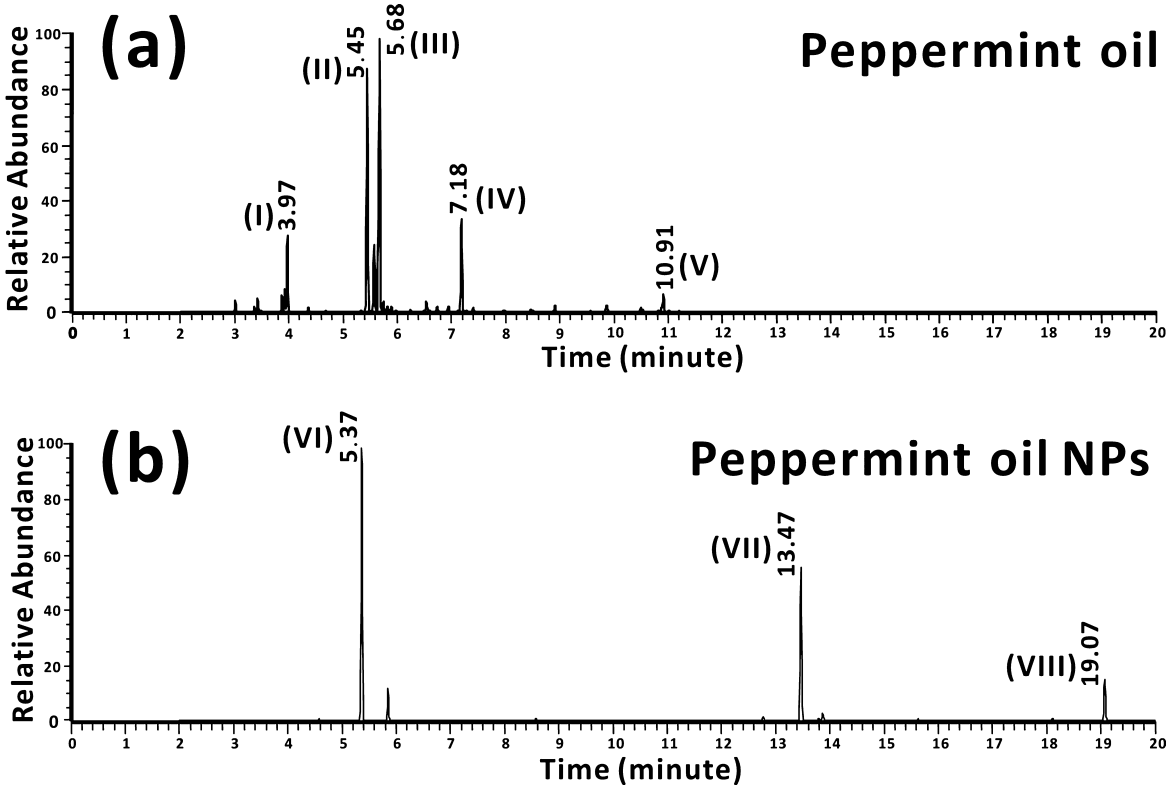

Figure 3. GC/MS total ion chromatograms from pure peppermint oil (a) and peppermint oil NP (b) samples also described in Table 1.

dx.doi.org/10.1021/sc500242k | ACS Sustainable Chem. Eng. 2014, 2, 1769–1775

Table 1. Chemical Composition of Peppermint Oil and Peppermint oil NPs by GC/MS

peak	constituents	[a]RT (min)	[b]area (%)	[c]mass range (m/z)
Peppermint oil				
I	1,8-cineole	3.97	10.7	(154), 93, 81, 43, 139, 69, 108, 41,55
II	menthone	5.45	25.9	(154), 139, 97, 41, 84, 112, 69, 55, 155
III	menthol	5.68	44.9	(156), 139, 123, 109, 95, 81, 79, 67, 55, 43, 41
IV	pulegone	7.18	9.7	(152), 138, 123, 109, 95, 81, 79. 67, 55, 43, 41
V	caryophyllcne	10.91	2.6	(204), 205, 187, 161, 133, 119, 105, 91,79, 67, 55, 43, 41
Peppermint oil NPs				
VI	diphenylmethane	5.37	49.3	(167), 167, 137, 107,91
VII	1,3,3,4′,6- pentamethyl-2,3,5,6,7,8-hexahydrospiro[2,4a-epoxynaphthalene-4,l′-cyclohexan]-2′-one	13.47	31.6	(303), 303, 273, 241, 211, 165, 138, 91
VIII	1,3,3,4′,6-pentamethyl-2′-((5-methyl-2-(propan-2-ylidene)cyclohexyl)oxy)-2,3,5,6,7,8-hexahydrospiro[2,4a-epoxynaphtlialene-4,l′-cyclohexane]	19.07	8.9	(439), 439, 407, 377, 361, 329, 315, 299, 269, 239, 196, 91

[a]RT (min): Retention time obtained by chromatogram. [b]Area (%) was determined by GC/MS. [c]Mass range (m/z) was determined by mass spectrometry.

diphenylmethane (compound VI) was formed from 1,8-clineole (compound I) via a serial of dehydration and dehydroxylation. The cyclization of pulegone (compound IV) formed menthofuran, which could undergo a Diels–Alder reaction with pulegone to form compound VII. Finally, compound VIII is presumed to be formed by compound VII and pulegone (compound IV). These compounds are identified in Table 1.

X-ray photoelectron spectra indicated that the peppermint oil NPs were composed of oxygen and carbon as shown in Figure 4a and b. The O 1s spectrum exhibited a single peak at 534 eV (Figure 4a), which is attributed to carboxyl group O–C=O,[27] and the C 1s spectrum had one peak at 286.6 eV, which can be fit to three peaks at 286.6, 287.8, and 290.7 eV, which are assigned to C–O, C=O, and –COO species, respectively (Figure 4b).[24,28] The peppermint oil NP FTIR spectrum (Figure 4c) showed characteristic bands associated with methyl and methylene groups, with peaks at 2954 cm^{-1} ($-CH_3$ asymmetric stretching), 2931 cm^{-1} ($-CH_2$ asymmetric stretching), 2869 cm^{-1} ($-CH_3$ symmetric stretching), and a peak at 1712 cm^{-1}, which is representative of the C=O stretch.[29] Together, the XPS and FTIR results shown in Figure 4 suggest the presence of a variety of functional groups on the surface of the peppermint oil NPs including C=O, C–O, and –CH, which may contribute to a series of fluorescent emissive traps between $\pi-\pi^*$ states.[24]

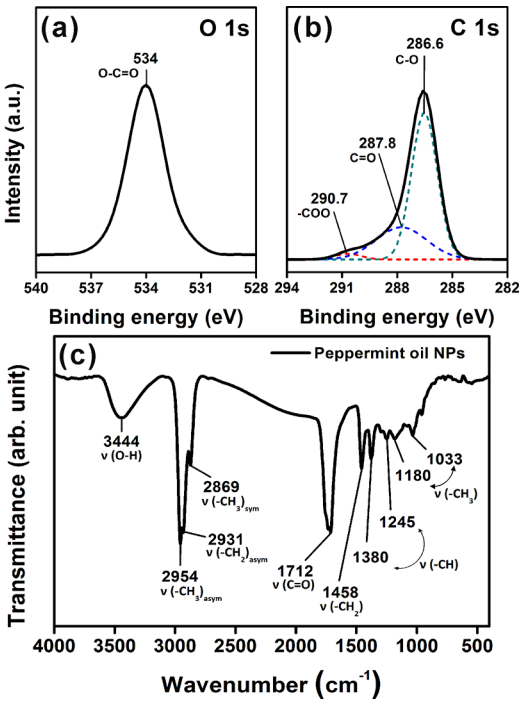

Figure 4. Elemental and chemical analyses of peppermint oil NPs using XPS and FTIR. XPS data of particles deposited on silicon substrate, showing (a) O 1s and (b) C 1s binding energy peaks. (c) FTIR spectra showed peaks at 2954 cm^{-1} ($-CH_3$ asymmetric stretching), 2931 cm^{-1} ($-CH_2$ asymmetric stretching), 2869 cm^{-1} ($-CH_3$ symmetric stretching), and 1712 cm^{-1} (C=O stretching), indicating the presence of methyl and methylene groups.

Inhibition Effect of Peppermint Oil NPs on Bacterial Growth. Peppermint oil has been shown to inhibit the growth of bacteria such as Gram-positive cocci and rods and Gram-negative rods[30,31] and has a bactericidal activity against pathogenic bacteria, including *E. coli* 015:H7, *H. pylori*, and *S. enteritidis*.[32] Here, we compare the effects of peppermint oil and peppermint oil NPs on the colony formation behavior of the bacteria *E. coli*.

Figure 5 shows the effects of increasing peppermint oil and peppermint oil NP preincubation concentrations on the subsequent growth of *E. coli* colonies on an LB agar plate. Here, the peppermint oil NPs (Figure 5f,g,h) exhibited much better bacterial growth inhibition than peppermint oil (Figure 5b,c,d). Even with a low dose of 5% peppermint oil NPs, an obvious decrease in colony density was observed (Figure 5f). Conversely, no significant colony formation inhibition was observed for the peppermint oil group at the 5% dose (Figure 5b). Further, the peppermint oil NPs exhibited a much higher bactericidal activity at 10% (Figure 5g) compared with the peppermint oil group (Figure 5c). At the highest concentration (25%), both groups exhibited strong bacterial growth inhibition.

The colony forming units were further counted and compared, and the resulting histogram as shown in Figure 6. When *E. coli* was treated with 5% peppermint oil and peppermint oil NPs for 16 h, the cfu inhibition efficiency reached 70 ± 3.0% and 99 ± 0.2%, respectively. Furthermore, peppermint oil NPs revealed full cfu inhibition (100%) at a 10% concentration treatment. These results indicate that peppermint oil NPs have superior bactericidal performance over normal peppermint oil.

Fluorescence Images of *E. coli* Labeled with Peppermint Oil NPs. To evaluate the NP photoluminescence properties, we treated *E. coli* cells with peppermint oil NPs, peppermint oil, and glycerol for 3 h, and then prepared samples of each on microscope slides to acquire fluorescence

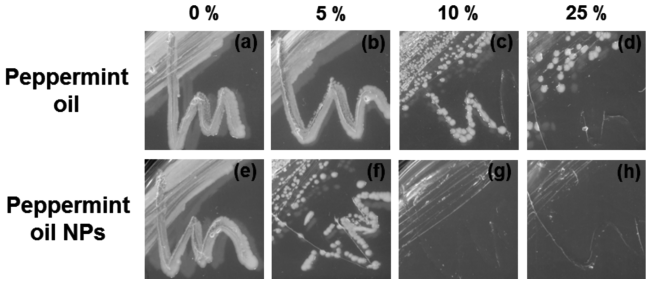

Figure 5. Colony growth inhibition of *E. coli* by peppermint oil NPs using streaking pattern assay. Bacteria (2×10^6 cfu/mL) were preincubated with 0%, 5%, 10%, and 25% peppermint oil and peppermint oil NPs for 3 h at room temperature. The bacterial cells were then grown on an LB agar plate overnight at 37 °C in an incubator.

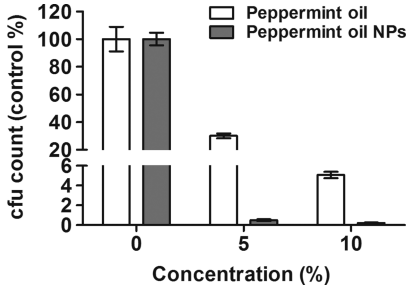

Figure 6. Comparison of colony forming unit (cfu) count among *E. coli* after treatment with peppermint oil and peppermint oil NPs. Bacteria were incubated with peppermint oil and peppermint oil NPs and grown on LB agar plates for 16 h at 37 °C in an incubator. The numbers of colonies formed were counted and plotted in the graph as a function of concentration. The peppermint oil-treated samples exhibited some cfu inhibition; however, the NP-treated samples strongly inhibited the cfu, with nearly 100% inhibition at 5% and 10% concentrations.

images (Figure 7). The images clearly show that the *E. coli* cells incubated with peppermint oil NPs exhibited much brighter blue and green fluorescence (Figure 7c and f, respectively) compared to those incubated with glycerol (Figure 7a and d) or with peppermint oil (Figure 7b and e). The photoluminescence measurements were conducted using two excitation wavelengths (359 and 499 nm) with corresponding long-pass filters for detection (461 and 520 nm, respectively). These results indicate that peppermint oil NPs can be very effective as bioimaging probes.

Antibacterial Activity of Peppermint Oil NPs. The antimicrobial efficacy of the pure peppermint oil and peppermint oil NPs was tested using *E. coli* bacteria (Figure 8). Preliminary screening revealed that the as-synthesized peppermint oil NPs showed much greater antimicrobial activity compared to pure peppermint oil in the same proportions. At the highest concentrations, (25%), peppermint oil NPs exhibited nearly 2-fold greater antimicrobial activity compared to peppermint oil as measured using the Kirby–Bauer disc diffusion test (zone diameter was 20.50 ± 1.20 mm vs 11.06 ± 0.68 mm, respectively). The complete results for this test are shown in Table 2.

Peppermint has been reported to provide the benefits of antibacterial activity and medicinal value.[33,34] The principal active constituents of peppermint are the essential oils, which are dominated by monoterpenes, mainly menthol, menthone, and their derivatives such as isomenthone, neomenthol, acetylmenthol, and pulegone. These essential oils dilate peripheral blood vessels and inhibit bacteria growth. Peppermint oils, especially menthol, have broad spectrum antibacterial activity because Gram-positive and Gram-negative bacteria were found susceptible to the oils.[31]

After heat treatment of the peppermint oil to form NPs, three new larger compounds were observed in GC/MS spectra (Figure 3). These new compounds were likely formed from several of the active peppermint oil constituents such as 1,8-clineole and pulegone, etc. (Table 1), which have demonstrated antimicrobial activity,[3335,] and may contribute and enhance the antibacterial properties of the resulting peppermint oil NPs.

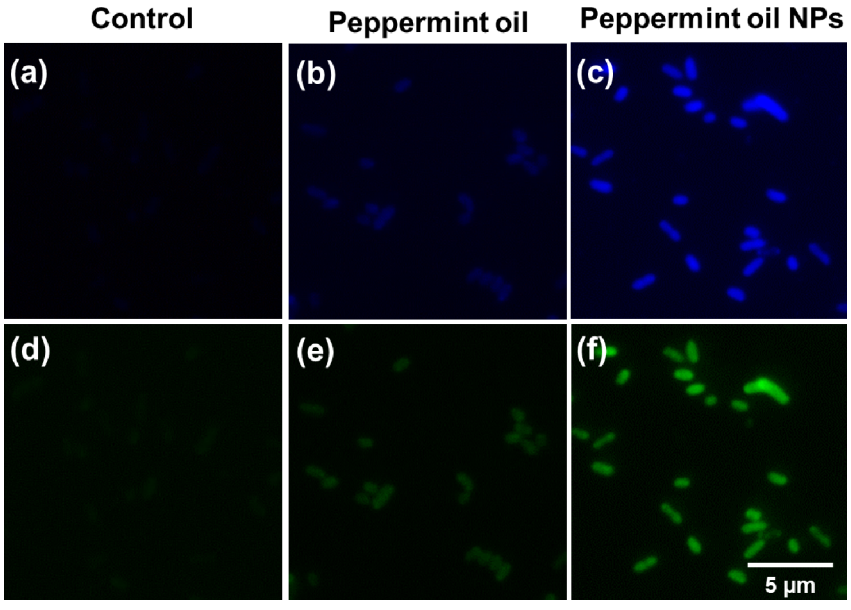

Figure 7. Fluorescence images of treated *E. coli* cells. (a,b,c) λex = 359 nm, detected with 461 nm long-pass filter. (d,e,f) λex = 499 nm, detected with 520 nm long-pass filter. *E. coli* cells (approximately 10^8 cfu/mL) were treated with 10% glycerol (as a control) (a,d), peppermint oil (b,e), and peppermint oil NP suspension (c,f) for 3 h at room temperature. *E. coli* cells treated with peppermint oil NPs exhibited bright blue and green luminescence compared to the control and peppermint oil groups.

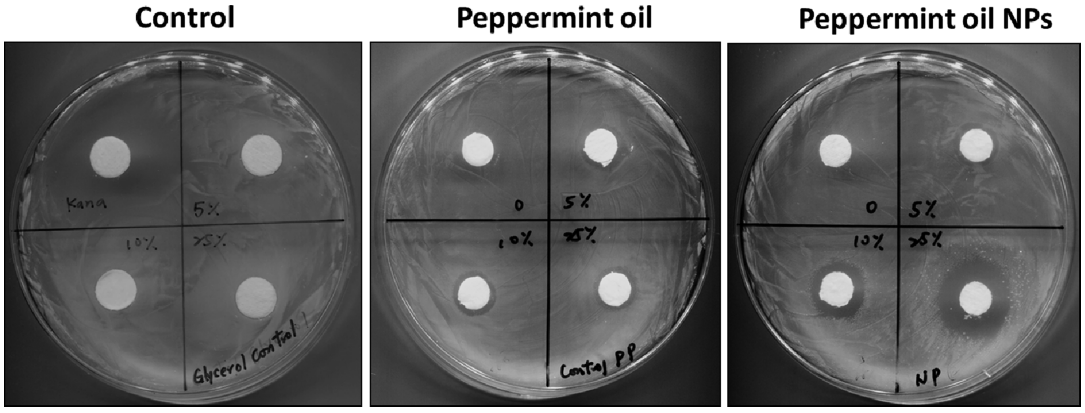

Figure 8. Antimicrobial efficacy of the as-synthesized peppermint oil NPs determined using the Kirby–Bauer disc diffusion test.

Table 2. Zone Inhibition Measurements Using the Kirby–Bauer Disc Diffusion Test To Assess the Antibacterial Activity of Peppermint Oil NPs

	Inhibitory activity (mm)[a]			
	0%	5%	10%	25%
glycerol	–	–	–	–
peppermint oil	–	10.06 ± 0.68	10.88 ± 0.64	11.06 ± 0.68
peppermint oil NPs	–	10.94 ± 0.86	13.31 + 1.22	20.50 + 1.20
kanamycin (50 mg/mL)	31.13 ± 2.59			

[a]Each value is the mean of three replicates of the diameter (mm) of the inhibition zone in the bacterial layer. Values are mean of three independent experiments.

The antibacterial activity of the peppermint oil NPs may be attributed to (a) size effects (Figure 1) (the NPs were 1.5 ± 0.5 nm, which facilitates ease of cell membrane penetration), (b) the new compounds may have a higher affinity toward the bacterial cell membrane and interact strongly with intracellular sites (which is critical for antibacterial activity), or (c) enhanced antimicrobial effects of the new compounds (Figure 3) and monoterpenes, such as menthol, by a perturbation of the lipid fraction of bacterial plasma membrane, resulting in alterations of membrane permeability and in leakage of intracellular materials.[34]

The peppermint essential oils contain a mixture of different chemical compounds. When the peppermint oil was heated to form NPs, three new larger compounds were formed. It is difficult to attribute the biological activities of peppermint oil NPs to a simple single component or mechanism. In addition to the major compounds, minor compounds may also contribute significantly to the oil's antibacterial activity.[36] However, it is clear that the peppermint oil NPs exhibited a significant change in fluorescence properties as well as a nearly 2-fold enhancement in antibacterial activity (at 25%) by simply heating the peppermint oil at 120 °C for 1 h.

CONCLUSIONS

Peppermint oil NPs were synthesized using a simple and economical one-pot method. No chemical agents or organic solvents were used in the process, thus minimizing any hazardous impact on human health and the environment. Further, peppermint oil is an environmentally benign substance that is safe and easily obtained, making it an affordable and readily available resource for producing NPs. The derived NPs exhibited both strong antibacterial activity and multicolor fluorescence in *E. coli* testing, thus demonstrating their bifunctionality as agents for bactericidal and bioimaging applications. This type of dual purpose NP may lead to new strategies for bacterial disease treatment and hygienic device coatings and to further advances in the fields of microbiology and biomedical research.

ASSOCIATED CONTENT

Supporting Information

Particle size distribution by histogram analysis of AFM data. This material is available free of charge via the Internet at http://pubs.acs.org.

AUTHOR INFORMATION

Corresponding Author

*Tel: 011-886-7-525-2000, ext. 3931. Fax: 011-886-7-525-3908. E-mail: shsieh@mail.nsysu.edu.tw.

Notes

The authors declare no competing financial interest.

ACKNOWLEDGMENTS

The authors thank the Ministry of Science and Technology (NSC 101-2113-M-110-013-MY3) of Taiwan, NSYSU-KMU Joint Research Project (NSYSUKMU 2013-P008), Kaohsiung Medical University Center for Stem Cell Research, and National Sun Yat-sen University Biochip Research Group for financial support of this work. Prof. Hsieh also thanks Dr. David Beck and Dr. Jiin-Tsuey Cheng for helpful discussions.

REFERENCES

(1) Siddhartha, S.; Tanmay, B.; Arnab, R.; Gajendra, S.; Ramachandrarao, P.; Debabrata, D. Characterization of enhanced antibacterial effects of novel silver nanoparticles. *Nanotechnology* **2007**, *18*, 225103.

(2) De Jong, W. H.; Borm, P. J. Drug delivery and nanoparticles: applications and hazards. *Int. J. Nanomed.* **2008**, *3*, 133–149.

(3) Vaseashta, A.; Dimova-Malinovska, D. Nanostructured and nanoscale devices, sensors and detectors. *Sci. Technol. Adv. Mater.* **2005**, *6*, 312–318.

(4) Lin, P. Y.; Hsieh, C. W.; Kung, M. L.; Hsieh, S. Substrate-free self-assembled SiOx-core nanodots from alkylalkoxysilane as a multicolor photoluminescence source for intravital imaging. *Sci. Rep.* **2013**, *3*, 1703.

(5) Gajjar, P.; Pettee, B.; Britt, D. W.; Huang, W.; Johnson, W. P.; Anderson, A. J. Antimicrobial activities of commercial nanoparticles against an environmental soil microbe, *Pseudomonas putida* KT2440. *J. Biol. Eng.* **2009**, *3*, 9.

(6) Prodan, A. M.; Iconaru, S. L.; Chifiriuc, C. M.; Bleotu, C.; Ciobanu, C. S.; Motelica-Heino, M.; Sizaret, S.; Predoi, D. Magnetic properties

and biological activity evaluation of iron oxide nanoparticles. *J. Nanomater.* **2013**, 7.
(7) Azam, A.; Ahmed, A. S.; Oves, M.; Khan, M. S.; Habib, S. S.; Memic, A. Antimicrobial activity of metal oxide nanoparticles against Gram-positive and Gram-negative bacteria: a comparative study. *Int. J. Nanomed.* **2012**, *7*, 6003−6009.
(8) Joshi, P.; Chakraborti, S.; Chakrabarti, P.; Haranath, D.; Shanker, V.; Ansari, Z. A.; Singh, S. P.; Guptas, V. Role of surface adsorbed anionic species in antibacterial activity of ZnO quantum dots against *Escherichia coli*. *J. Nanosci. Nanotechnol.* **2009**, *9*, 6427−6433.
(9) Lu, Z.; Li, C. M.; Bao, H.; Qiao, Y.; Toh, Y.; Yang, X. Mechanism of antimicrobial activity of CdTe quantum dots. *Langmuir* **2008**, *24*, 5445−5452.
(10) Luo, Z.; Wu, Q.; Zhang, M.; Li, P.; Ding, Y. Cooperative antimicrobial activity of CdTe quantum dots with rocephin and fluorescence monitoring for *Escherichia coli*. *J. Colloid Interface Sci.* **2011**, *362*, 100−106.
(11) Iwalokun, B. A.; Ogunledun, A.; Ogbolu, D. O.; Bamiro, S. B.; Jimi-Omojola, J. In vitro antimicrobial properties of aqueous garlic extract against multidrug-resistant bacteria and Candida species from Nigeria. *J. Med. Food* **2004**, *7*, 327−333.
(12) Prabuseenivasan, S.; Jayakumar, M.; Ignacimuthu, S. In vitro antibacterial activity of some plant essential oils. *BMC Complementary Altern. Med.* **2006**, *6*.
(13) Aridogan, B. C.; Baydar, H.; Kaya, S.; Demirci, M.; Ozbasar, D.; Mumcu, E. Antimicrobial activity and chemical composition of some essential oils. *Arch. Pharm. Res.* **2002**, *25*, 860−864.
(14) Yoshimura, K.; Yamagishi, T. Immunologic response of guinea pigs to infection with Angiostronglyus cantonensis. *Nihon Juigaku Zasshi* **1975**, *37*, 585−591.
(15) Subash Babu, P.; Prabuseenivasan, S.; Ignacimuthu, S. Cinnamaldehyde-A potential antidiabetic agent. *Phytomedicine* **2007**, *14*, 15−22.
(16) Singh, S.; Majumdar, D. K. Effect of *Ocimum sanctum* fixed oil on vascular permeability and leucocytes migration. *Indian J. Exp. Biol.* **1999**, *37*, 1136−1138.
(17) Kumar, A.; Samarth, R. M.; Yasmeen, S.; Sharma, A.; Sugahara, T.; Terado, T.; Kimura, H. Anticancer and radioprotective potentials of *Mentha piperita*. *BioFactors* **2004**, *22*, 87−91.
(18) Arias, B. Á.; Ramón-Laca, L. Pharmacological properties of citrus and their ancient and medieval uses in the Mediterranean region. *J. Ethnopharmacol.* **2005**, *97*, 89−95.
(19) Boschi, F.; Fontanella, M.; Calderan, L.; Sbarbati, A. Luminescence and fluorescence of essential oils. Fluorescence imaging in vivo of wild chamomile oil. *Eur. J. Histochem.* **2011**, *55*, e18.
(20) Alankar, S. A review on peppermint oil. *Asian J. Pharm. Clin. Res.* **2009**, *2*, 7.
(21) Choi, H. S.; Liu, W.; Misra, P.; Tanaka, E.; Zimmer, J. P.; Ipe, B. I.; Bawendi, M. G.; Frangioni, J. V. Renal clearance of quantum dots. *Nat. Biotechnol.* **2007**, *25*, 6.
(22) De, B.; Karak, N. A green and facile approach for the synthesis of water soluble fluorescent carbon dots from banana juice. *RSC Adv.* **2013**, *3*, 8286−8290.
(23) Mochalin, V. N.; Gogotsi, Y. Wet chemistry route to hydrophobic blue fluorescent nanodiamond. *J. Am. Chem. Soc.* **2009**, *131*, 4594−4595.
(24) Sahu, S.; Behera, B.; Maiti, T. K.; Mohapatra, S. Simple one-step synthesis of highly luminescent carbon dots from orange juice: Application as excellent bio-imaging agents. *Chem. Commun.* **2012**, *48*, 8835−8837.
(25) Zhu, S.; Zhang, J.; Qiao, C.; Tang, S.; Li, Y.; Yuan, W.; Li, B.; Tian, L.; Liu, F.; Hu, R.; Gao, H.; Wei, H.; Zhang, H.; Sun, H.; Yang, B. Strongly green-photoluminescent graphene quantum dots for bioimaging applications. *Chem. Commun.* **2011**, *47*, 6858−6860.
(26) Iscan, G.; Kirimer, N.; Kurkcuoglu, M.; Baser, K. H.; Demirci, F. Antimicrobial screening of *Mentha piperita* essential oils. *J. Agric. Food Chem.* **2002**, *50*, 3943−3946.
(27) Kumar, S.; Tong, X.; Dory, Y. L.; Lepage, M.; Zhao, Y. A CO_2-switchable polymer brush for reversible capture and release of proteins. *Chem. Commun.* **2013**, *49*, 90−92.
(28) Zhu, C.; Zhai, J.; Dong, S. Bifunctional fluorescent carbon nanodots: Green synthesis via soy milk and application as metal-free electrocatalysts for oxygen reduction. *Chem. Commun.* **2012**, *48*, 9367−9369.
(29) Petrakis, E. A.; Kimbaris, A. C.; Pappas, C. S.; Tarantilis, P. A.; Polissiou, M. G. Quantitative determination of pulegone in pennyroyal oil by FT-IR spectroscopy. *J. Agr. Food Chem.* **2009**, *57*, 10044−10048.
(30) Pattnaik, S.; Subramanyam, V. R.; Kole, C. Antibacterial and antifungal activity of ten essential oils in vitro. *Microbios* **1996**, *86*, 237−246.
(31) Pattnaik, S.; Subramanyam, V. R.; Bapaji, M.; Kole, C. R. Antibacterial and antifungal activity of aromatic constituents of essential oils. *Microbios* **1997**, *89*, 39−46.
(32) Imai, H.; Osawa, K.; Yasuda, H.; Hamashima, H.; Arai, T.; Sasatsu, M. Inhibition by the essential oils of peppermint and spearmint of the growth of pathogenic bacteria. *Microbios* **2001**, *106* (Suppl 1), 31−39.
(33) Duru, M. E.; Ozturk, M.; Ugur, A.; Ceylan, O. The constituents of essential oil and in vitro antimicrobial activity of *Micromeria cilicica* from Turkey. *J. Ethnopharmacol.* **2004**, *94*, 43−48.
(34) Trombetta, D.; Castelli, F.; Sarpietro, M. G.; Venuti, V.; Cristani, M.; Daniele, C.; Saija, A.; Mazzanti, G.; Bisignano, G. Mechanisms of antibacterial action of three monoterpenes. *Antimicrob. Agents Chemother.* **2005**, *49*, 2474−2478.
(35) Randrianarivelo, R.; Sarter, S.; Odoux, E.; Brat, P.; Lebrun, M.; Romestand, B.; Menut, C.; Andrianoelisoa, H. S.; Raherimandimby, M.; Danthu, P. Composition and antimicrobial activity of essential oils of *Cinnamosma fragrans*. *Food Chem.* **2009**, *114*, 680−684.
(36) Wang, W.; Wu, N.; Zu, Y. G.; Fu, Y. J. Antioxidative activity of *Rosmarinus officinalis* L. essential oil compared to its main components. *Food Chem.* **2008**, *108*, 1019−1022.